



SPE 75246

Geological characterization of naturally fractured reservoirs using multiple point geostatistics

Xiaohuan Liu, Sanjay Srinivasan (Univ. of Calgary) and Dale Wong (Object Reservoirs Inc.)

Copyright 2002, Society of Petroleum Engineers Inc.

This paper was prepared for presentation at the SPE/DOE Thirteenth Symposium on Improved Oil Recovery held in Tulsa, Oklahoma, 13–17 April 2002.

This paper was selected for presentation by an SPE Program Committee following review of information contained in an abstract submitted by the author(s). Contents of the paper, as presented, have not been reviewed by the Society of Petroleum Engineers and are subject to correction by the author(s). The material, as presented, does not necessarily reflect any position of the Society of Petroleum Engineers, its officers, or members. Papers presented at SPE meetings are subject to publication review by Editorial Committees of the Society of Petroleum Engineers. Electronic reproduction, distribution, or storage of any part of this paper for commercial purposes without the written consent of the Society of Petroleum Engineers is prohibited. Permission to reproduce in print is restricted to an abstract of not more than 300 words; illustrations may not be copied. The abstract must contain conspicuous acknowledgment of where and by whom the paper was presented. Write Librarian, SPE, P.O. Box 833836, Richardson, TX 75083-3836, U.S.A., fax 01-972-952-9435.

Abstract

The spatial distribution of fractures in a reservoir affects the displacement of fluids and the prediction of future performance. Realistic characterization of fractured reservoirs requires quantification and classification of fracture patterns on the basis of the underlying geological characteristics and developing reservoir modeling algorithms that can integrate connectivity based (multiple point) statistics related to fracture patterns. A methodology for summarizing the characteristics of fracture networks based on multiple point connectivity functions is presented. The paper also presents a stochastic simulation methodology for constraining the target reservoir model to the connectivity characteristics derived from analog models and to all other available reservoir specific data in the form of well information and seismic areal proportion maps.

Introduction

A natural fracture is a planar discontinuity in reservoir rock due to deformation or physical diagenesis¹. Fractures may have either a positive or negative effect on fluid flow depending on whether they are open or sealed due to mineralization. For the purposes of this paper, a fractured reservoir is defined as a reservoir in which naturally occurring fractures are predicted to have a significant effect on fluid flow either in the form of increased permeability and/or porosity or increased permeability anisotropy.

Natural fracture patterns are frequently interpreted on the basis of laboratory-derived fracture patterns corresponding to models of paleo-stress fields and strain distribution in the reservoir at the time of fracture². Stearns and Friedman³ proposed a genetic classification of fracture systems based on stress/strain conditions in laboratory samples and features observed in outcrops and sub-surface settings. Based on their work, fractures are generically classified into:

Shear Fractures - exhibit a sense of displacement parallel to the fracture plane. Shear fractures form when the stresses in the three principal directions are all compressive. They form at an acute angle to the maximum principal stress direction and at an obtuse angle to the minimum compressive stress direction.

Extension Fractures - exhibit a sense of displacement perpendicular to and away from the fracture plane. They form perpendicular to the minimum stress direction. They too result when the stresses in the three principal directions are compressive and can occur in conjunction with shear fractures.

Tension Fractures - Exhibit a sense of displacement perpendicular to and away from the fracture plane. However, in order to form a tension fracture, at least one of the principal stresses has to be tensile. Since rocks exhibit significantly reduced strength in tension tests, the frequency of fractures under tensile stress conditions is more.

The geologic classification of fracture systems is based on the assumption that natural fractures depict the paleo-stress conditions in the reservoir at the time of fracturing. Based on geologic conditions, fractures can be classified as:

Tectonic fractures - The orientation, distribution and morphology of these fracture systems are associated with local tectonic events. Tectonic fractures form in networks with specific spatial relationships to faults and folds. Fault-related fracture systems could be shear fractures formed either parallel to the fault or at an acute angle to the fault or in the case of a fault-wedge, they can be extension fractures bisecting the acute angle

between the two fault shear directions^{4,5}. The intensity of fractures associated with faulting is a function of lithology, distance from the fault plane, magnitude of fault displacement, total strain in the rock mass and depth of burial.

Fold-related fracture systems exhibit complex patterns consistent with the complex strain and stress history associated with the initiation and growth of a fold^{6,7}. Fracture types in fold-related systems are defined in terms of the dip and strike of the beds.

Regional Fractures - These fracture systems are characterized by long fractures exhibiting little change in orientation over their length. The fractures also show no evidence of offset across the fracture plane and are always perpendicular to the bedding surfaces⁸. Regional fracture systems can be distinguished from tectonic fractures in that they generally exhibit simpler and more consistent geometry and have relatively larger spacing.

Regional fractures are commonly developed as orthogonal sets with the two orthogonal orientations parallel to the long and short axis of the basin in which the fractures are formed⁹. Many theories have been proposed for the origin of natural fractures, ranging from plate tectonics to cyclic loading/unloading of rocks associated with earth tides. As in the case of tectonic fractures, small-scale variations in regional fracture orientation of up to $\pm 20^\circ$ can result due to strength anisotropies in reservoir rocks due to sedimentary features such as cross-bedding.

Contractional Fracture - These are fractures that result due to bulk volume reduction of the rock. Desiccation fractures may result due to shrinkage upon loss of water in sub-aerial drying. Mud cracks are the most common fractures of this type¹⁰. Syneresis fractures result from bulk volume reduction within sediments by sub-aqueous or subsurface dewatering. Dewatering and volume reduction of clays or of a gel or of colloidal suspension can result in syneresis fractures. Desiccation and syneresis fractures can be either tensile or extension fractures and are initiated by internal body forces. The fractures tend to be closely spaced and regular and isotropically distributed in three dimensions. Syneresis fractures have been observed in limestones, dolomites, shales and sandstones¹¹.

Thermal contractional fractures may result due to contraction of hot rock as it cools. Depending on the depth of burial they may be either tensile or extension fractures. The generation of thermal fractures is predicated on the existence of thermal gradient within the reservoir rock material. A classic example of thermally induced fracture is the columnar jointing

observed in igneous rocks¹². Fractures may also result due to mineral phase change in carbonates and clay constituents in sedimentary rocks. Phase changes such as the chemical change from calcite to dolomite result in changes in bulk volume and this leads to complex fracture patterns.

As seen from the above discussion, complex stress and strain distributions in reservoir rocks result in complex fracture patterns. Fracture patterns corresponding to different geological systems have key characteristics that can be used to classify and index fracture networks observed in outcrops and subsurface samples.

Problem Statement

In order to develop a robust reservoir model representative of the target reservoir, it is necessary to first understand the geological conditions leading to the development of fractures in the reservoir rock. Once the geological context for the origin and propagation of fractures is understood, the fracture pattern corresponding to that geological scenario can be postulated from analogs such as outcrops, laboratory models etc. These spatial fracture patterns have to be imposed on models for the target reservoir while at the same time honoring conditioning data in the form of well samples, dipmeter surveys, seismic maps and production data.

The development of a set of tools that facilitate the development of constrained fractured reservoir models is the primary objective of this paper. Fracture patterns corresponding to key geological fracture types are recognized using spatial connectivity measures. These patterns are imposed on a reservoir model while at the same time honoring conditioning data using a stochastic simulation algorithm.

Recognition of fracture patterns

Fracture patterns are generally characterized by statistics such as fracture spacing, density, orientation and statistical distributions of width. Differences in variation of fracture orientations and spacing are important for distinguishing between different fracture types as discussed previously. Data for inferring distributions of orientation, spacing and density are generally obtained after detailed outcrop characterization. Figure 1 depicts the regional fracture patterns found in Jurassic Navajo sandstone, Lake Powell, southeastern Utah¹³. The dominant fracture orientation can be gauged visually in that figure. Figure 2 depicts a set of conjugate shear fractures in an outcrop from Wyoming. This set is reflective of tectonic fractures. Figure 3 is a photograph of desiccation cracks observed

in mud¹⁴. It is evident that the three fracture systems exhibit widely different pattern characteristics. These characteristics are explored in terms of spatial connectivity measures.

Indicator Variograms

Two-point statistics computed using indicator variables are an effective tool for visualizing the spatial connectivity of fractures. Defining an indicator as:

$$I(\mathbf{u}) = \begin{cases} 1, & \text{if } \mathbf{u} \in \text{fracture} \\ 0, & \text{otherwise} \end{cases} \quad (1)$$

\mathbf{u} represents a location within the reservoir.

The indicator semi-variogram¹⁵ is defined as:

$$\gamma_I(\mathbf{h}) = \frac{1}{2} \cdot E \left\{ (I(\mathbf{u}) - I(\mathbf{u} + \mathbf{h}))^2 \right\} \quad (2)$$

The indicator variogram is a measure of the proportion of pairs in which $I(\mathbf{u}) = 1$ and $I(\mathbf{u} + \mathbf{h}) = 0$ or vice-versa. In other words, the indicator variogram is a measure of the probability of transition from the rock matrix to fracture and vice-versa. Figure 4 shows the indicator variogram corresponding to regional, tectonic and contractional fractures computed in the x and y directions. Figure 5 shows rose diagrams summarizing the variation in variogram ranges in different directions. The predominance of regional fractures in the North-South and East-West directions is emphasized. Shear fractures show maximum continuity in the 45° and 135° directions. Desiccation fractures exhibit isotropy and the maximum range of continuity is smaller than that for the other two systems.

Multiple point connectivity function

The indicator variogram/covariance concept can be extended to more than 2 points. An N-order connectivity function that measures the frequency of N connected voxels jointly within a fracture is a multiple-point statistic. Mathematically, a spatial connectivity measure associated to N-points separated by the same lag separation vector \mathbf{h} can be defined as follows^{16,17}:

$$\varphi_N(\mathbf{h}) = E \left\{ \prod_{j=1}^N I(\mathbf{u} + (j-1) \cdot \mathbf{h}) \right\} \quad (3)$$

For N=2, Equation 3 reduces to the non-centered indicator covariance¹⁵. In general for an N-point template, the multiple point product is non-zero only if all N points on the template are jointly within the fracture. Figure 6 shows the connectivity functions corresponding to the three fracture systems calculated in different

directions. The connectivity function for the regional fracture case decreases more gradually in the 90° (y) direction indicating maximum continuity in that direction. The difference in continuity in different directions is illustrated more clearly in Figure 7. These figures plot the template size corresponding to which the connectivity function value decreases to 10% of the value corresponding to N=1 (which is the proportion of pixels classified as fracture). Thus based on Figure 7 it can be concluded that the regional fracture system has a predominant North-South orientation, but there is connectivity in the East-West direction also. The shear fracture system shows two dominant orientations, in the 45° and 150° directions. The desiccation fractures do not exhibit any dominant orientation.

Multiple point Histograms

The concept of multi-point histograms¹⁷ can be used to summarize the multi-point characteristics exhibited by the geological system. Consider a categorical variable that takes outcomes $k = 1, \dots, K$. The multi-point histogram corresponding to an N-point geometric template, measures the frequency of occurrence of each configuration of K categories within the template. Thus, given an N-point template with lag $\mathbf{h}_1, \dots, \mathbf{h}_N$ between the origin and all other nodes within the template and given K categories such that each node in the template has one of the K categories, the multipoint histogram denoted by:

$$f(\mathbf{h}_1, \dots, \mathbf{h}_N; k_1, \dots, k_N)$$

is the frequency of observing the particular combination of k_1, k_2, \dots, k_N categories at the N nodes.

The multiple point histogram is a complete measure of multiple point spatial connectivity. The previously defined indicator variogram and spatial connectivity function are simply multiple point histograms corresponding to specific spatial templates. The indicator variogram measures the frequency of an indicator category 1 at one node and 0 at the other node of a two point spatial template.

The multiple-point histogram for fracture systems can be computed for various geometric template configurations. Thus, if the data are indicator coded as either within a fracture or outside, there are 2 categories. Considering an N-point spatial template, each node of the template can have one of 2 categories, either 0 or 1. There are 2^N possible combinations of indicator values within the N point configuration. When the N-point template is translated over the reference fracture image, the spatial configuration of fracture on the template has to be one of the 2^N possible combinations.

An indexing scheme can be devised to systematically account for all possible combination of categories within the N-point template. Such an indexing scheme would be:

$$\text{index} = 1 + \sum_{i=1}^N [k_i - 1] \cdot K^{i-1} \quad (4)$$

K is the number of categories, 2 in this case. Thus, any configuration of data corresponds to one of the indices defined above. The frequency of a particular pattern recurring in the fracture model is computed by translating the N-point template over the reference fracture image and keeping track of the frequency corresponding to each index. Figure 9 shows the multiple point histogram corresponding to the three fracture systems using the spatial template shown in Figure 8. The histograms exhibit significantly different characteristics. All three histograms exhibit a peak at the index value of 1. This is simply the peak corresponding to the single-point statistic that is the proportion of fractures in the model. The histogram corresponding to the regional fracture system shows a strong second peak that indicates the predominance of patterns corresponding to that index. The histogram corresponding to the shear fracture system has a mean index of 2350. The histogram corresponding to the desiccation fracture also has a weak second peak and the mean index is close to 9000.

In order to understand the significance of these histograms and to relate them to the spatial patterns observed in the images, the pattern of fracture corresponding to the mean index for each histogram is plotted in Figure 10 a-c. The spatial pattern represented in Figure 10a represents the mean index (28870) for the first system. The predominance of North-South and East-West patterns of the regional fracture system is correctly reflected. Similarly, Figure 10b represents the pattern corresponding to the shear fracture system. The pattern corresponding to a pair of fractures oriented at an acute angle to each other is indicated. That would indicate a fracture system attributed to a normal fault. Desiccation fractures generally do not have a dominant orientation. The network of fractures exhibit a range of orientations and this is correctly captured in Figure 10c.

The results in this section indicate that the patterns corresponding to different classes of fracture systems can be described quantitatively using spatial connectivity measures. Two-point connectivity measures are adequate for capturing the general orientation of fractures. Details of the fracture pattern are better represented through multiple point connectivity functions such as the multiple point histogram. Thus, given the geological setting for a target reservoir, the connectivity

measures relevant for that setting can be retrieved and utilized to construct an analog model for the target reservoir. This analog model can be further adjusted to suit the geologist's prior view of the fracture system in the reservoir by making subtle adjustments to the connectivity measures.

Stochastic simulation

The analog reservoir model represents the geologist's prior vision of the fracture system that typifies the target reservoir. The prior model has to be subsequently conditioned to the available reservoir specific information. That information may be in the form of core measurements of fracture density, wireline logs indicative of changes in lithology, borehole images and sophisticated tools such as Formation MicroImager etc. Auxiliary information in the form of coarse resolution seismic images and well test data may also be available for the target reservoir. The next step in reservoir modeling is therefore to utilize the prior model for fracture patterns and constrain it to all the available information.

Since in most cases the data available to model the fractured reservoir is sparse and information such as seismic maps and production response are related imprecisely to the fracture pattern characteristics, a probabilistic approach to fracture characterization is necessary. In the object-based modeling approaches, fractures are represented as objects defined by their centroid, shape, size and orientation. In "Random Disk" models¹⁸, fractures are represented as two-dimensional convex circular disks located randomly in space. The radii of the disks are drawn from a lognormal distribution whose parameters are inferred from the fracture trace-length distributions observed in outcrops. The orientations of the disks are also drawn from a lognormal distribution and the disk locations, radii and orientation are assumed uncorrelated from one disk to the next. It is difficult to model the clustering of fractures accurately assuming random placement of disks. A spatial density function $\lambda(\mathbf{u})$ can be utilized to represent such clustering of fractures¹⁹. Seed locations for fractures are drawn based on this spatial density function and fracture sets are simulated over a pre-defined volume around the seed location. The resultant parent-daughter fracture sets exhibit clustering.

The conditioning of object-based fracture models to available well data is achieved by simply freezing the fractures at the well intersections, with the correct orientation and arbitrary fracture length. Although object-based models are easy to implement, their application is limited due to the assumed independence of the model parameters such as radii, orientation etc. In addition,

fractures are assumed to be planar and convex and consequently realistic depiction of undulations and distortions of fractures due to the presence of faults and variations in lithology is not possible. A viable alternative is to employ pixel-based algorithms. Well established geostatistical algorithms such as sequential indicator simulation (**sisim**)¹⁵ ensure reproduction of the two-point indicator variogram and can be used to classify nodes within the reservoir into fractures or matrix. However, it is evident from previous discussions that fracture patterns and connectivity are best represented through multiple point connectivity functions. Models constrained only to two-point statistics are generally noisy and consequently inadequate for capturing clean-cut shapes such as fractures.

The fundamental notion in pixel-based stochastic simulation is to derive the conditional probability distribution (ccdf) at each location within the reservoir given the surrounding data. That ccdf is written as:

$$\text{Prob}\{I(\mathbf{u}) = 1 \mid S(n)\} = E\{I(\mathbf{u}) = 1 \mid S(n)\} \quad (5)$$

\mathbf{u} is the simulation node and $S(n)$ is the surrounding data. Classification of the simulated node into fracture or matrix follows by drawing randomly from that ccdf. In the case of two-point statistics based algorithms that probability is calculated on the basis of two-point interaction between pairs of data and between each data and the unknown. In multiple point statistics based algorithms^{20,21} that conditional probability derived based on the entire data configuration, including the multi-point interactions among the data and between the data and the unknown. Supposing there are n neighboring data events $A_\alpha, \alpha = 1, \dots, n$. An additional variable $t(n)$

can be defined such that $t(n) = \prod_{i=1}^n A_\alpha$. Then $t(n) = 1$

only if all the elementary data events occur simultaneously i.e. $A_\alpha = 1, \forall \alpha = 1, \dots, n$. The previous conditional probability can be written as²¹:

$$\text{Prob}\{A_o = 1 \mid t(n) = 1\} = E\{A_o = 1 \mid t(n) = 1\} \quad (6)$$

A_o is the unknown data event at the unsampled location. In the case when the unknown data event is simply the indicator $I(\mathbf{u}) = 1$, then the expression (6) will simply be equal to the probability that the location \mathbf{u} will belong to category 1 (or fracture), given the multiple point configuration of data represented by the template $t(n)$. Using Bayes' rule, the conditional probability in expression (6) can be written as:

$$\text{Prob}\{A_o = 1 \mid t(n) = 1\} = \frac{\text{Prob}\{A_o = 1, t(n) = 1\}}{\text{Prob}\{t(n) = 1\}} \quad (7)$$

This implies that in order to derive the multiple point conditional probability expression (6), we need to know the joint probability of observing the spatial pattern $A_o = 1$ and $t(n) = 1$ as well as the prior probability of the occurrence of the template pattern $t(n) = 1$. These probabilities can be retrieved from the analog fracture model by scanning a template over the analog model. The joint frequency of events such that $A_o = 1$ and $t(n) = 1$ as well as the prior probability of the event $t(n) = 1$ can be retrieved. The ratio of the two yields the multiple point conditional probability corresponding to different events A_o . The simulated data event A_o^* is obtained by simply sampling from the conditional probability distribution.

Several researchers have utilized the notion of multiple point statistics to generate models of reservoirs with complex geometries. In most approaches^{20,17,22}, the simulation starts with a full grid of randomly distributed values drawn from a prior probability distribution. These values are iteratively perturbed, with the criteria for accepting the perturbation based on the conditional probabilities scanned from the analog model. In the case of optimization based approaches^{20,17} the criteria for stopping the iterations is based on the departure of the multiple point statistics computed on the simulated realization from the target statistics. An alternate multiple point approach starting from an empty grid and subsequently visiting each node sequentially along a random path is also possible²³. In that approach the multiple-point conditional probability distribution is scanned from the training image for all possible combination of conditioning events and stored. Then during the simulation phase, the configuration of data surrounding the simulation node is checked and the corresponding conditional probability is retrieved from the stored data. The simulated event (fracture or not) is obtained by sampling from the conditional probability distribution.

In contrast to all the above multiple point approaches, the proposed algorithm selects seed fracture locations based on areal proportion maps and subsequently grows a fracture from each seed location using the multiple point conditional probability inferred from analog fracture models as a criteria for growth. Such a growth algorithm has the advantage that it is computationally efficient and permits integration of other physical parameters such as fracture growth corresponding to variations in rock strength into the simulation.

Simulation Algorithm

The simulation commences from an empty grid. Then

each well location with recorded fracture data is visited sequentially. The data configuration on a 27-point template (Figure 11) surrounding the fracture location is examined. The location of neighbourhood points that are also in fractures is recorded. The analog fracture model is then scanned for the occurrence of that data configuration. Thus, if for example as in Figure 11, at the current stage of simulation, there are 23 points surrounding the central node that are in fracture, then the analog model is scanned for the occurrence of that 24-point (23 + 1 central node) data configuration. This represents the prior probability $\text{Prob}\{t(n)=1\}$. The data event A_o can then be one of the following:

- None of the remaining three points on the template is a fracture
- One of the remaining three locations is a fracture. That location could be any one of the remaining nodes
- Two of the remaining three locations are fractures. There are three possible combinations.
- All three of the remaining three locations are also fractures.

The probability associated with all such multiple point data events A_o is retrieved by scanning the analog model. This is the joint probability $\text{Prob}\{A_o = 1, t(n)=1\}$ corresponding to each data event A_o . The conditional probability: $\text{Prob}\{A_o = 1 | t(n)=1\}$ is then derived as the ratio of the joint probability and the prior probability. A random value is drawn from the conditional probability distribution and this yields the set of nodes corresponding to the outcome A_o^* that are marked as fractures for the next step of the simulation algorithm.

Remark

The treatment of A_o as an multiple point data event is an important departure from multiple point statistics based algorithms proposed earlier. In most algorithms proposed till date, the probability that the central node in an N-point template belongs to a certain category given the surrounding multiple point data event is inferred from the training image. This is equivalent to A_o being a single point data event i.e. $I(\mathbf{u})=1$ or 0.

Out of the n nodes corresponding to the n-point event, the node that has the smallest number of surrounding nodes that are fractures is chosen as the next node for growing the fracture. The algorithm proceeds with the growth process until a data event A_o with no additional nodes in fractures (corresponding to the first configuration above) is drawn as an outcome from the conditional probability distribution. The areal proportion map corresponding to the current stage of the simulation is computed. The conditional probabilities for the

simulation of the next fracture are multiplied by the ratio:

$$ratio = 1 - \frac{\text{prop}_{sim}}{\text{prop}_{target}}$$

This ratio ensures that the simulation honors the target proportion. In case the areal proportion map is available, the ratio is updated for each region using the target areal proportion and the simulation fracture proportion for that region. The next well conditioning data if available is used to seed the next fracture. In case no additional conditioning data are available and the simulated proportions are still lower than the target proportions, fracture seed locations are drawn based on the areal proportion map. The simulation is continued until the target proportions are matched in an ergodic sense.

Results

The simulation algorithm described above was implemented in 3-D. Since the analog fractured reservoir images in Figures 1-3 are in 2-D, a synthetic analog model mimicing a regional fracture system in 3-D was generated and used as a training model for the stochastic simulation. Sections through that 3-D training model in the X-Y, X-Z and Y-Z planes are shown in Figure 12. The analog model has dimensions of 50 x 50 x 10. The proportion of fractures in the model is 0.5 and the fractures were simulated using unconditional, Boolean simulation.

The simulation grid dimension was 100x100x10 and each block was 50mx50mx1m. Conditioning data for the simulation consisted of information along 20 wells. The wells were assumed to be vertical and cored over the entire interval. The template shown in Figure 11 was used to scan the training image and retrieve the multiple point conditional probabilities. The target global proportion of fractures was specified to be 20%.

Figure 13 shows slices through one simulated realization of fractures. The fracture patterns appear consistent with those observed in the training model. The vertical continuity of fracture planes observed in the training models is captured correctly in the simulated model. The simulation was repeated, this time with the areal proportion map shown in Figure 14. The resultant simulated model, also shown in Figure 14, reflects the increased density of fractures in areas consistent with the areal proportion map. The simulation algorithm also has the capability of integrating coarser resolution 3-D information such as 3-D seismic data.

Remarks

1. Gringarten²⁴ presented a growth-based algorithm for geometric modeling of fracture networks. That rule-based algorithm commences with an initial simulation

of fracture density on a coarse grid. Fractures are propagated between scan lines drawn on the coarse grid. If the number of fracture intersections with any scan line exceed the fracture density for that coarse block, fractures are terminated mid-way between the scan lines. Fractures are also terminated when unfavourable lithologies such as shale are encountered. That algorithm yields predominantly rectilinear fracture patterns and is difficult to implement in 3-D.

2. Wang²⁵ presented another growth-based algorithm. That algorithm based on the multiple point histogram (*mph*) commences from conditioning data locations. Candidate neighbouring locations for propagating the fracture on a spatial template are evaluated. A location is picked based on minimizing the deviation from the target *mph*. The neighbors of that new location together with the remaining eligible locations for the previous fracture node become candidate locations for the next phase of fracture growth. This accretion process continues until no significant reduction to the deviation from the target *mph* is observed. That algorithm differs from the one proposed for this research in that it is iterative and the simulation data event is still a single point event.

Discussion and Conclusions

This paper presents a methodology for generating stochastic models of fracture systems in reservoirs. The methodology hinges on the availability of training models of analogous fracture systems. It is demonstrated in this paper that salient characteristics of the patterns corresponding to different classes of fracture systems can be reliably detected using multiple point statistical measures. The proposal is therefore to perform detailed geological characterization of fracture outcrops. The essence of the fracture patterns depicted in those outcrop exposures can then be captured through multiple point statistical measures. Then, when modeling a target reservoir the analog model suitable for that reservoir can be constructed knowing the multiple-point statistical measures characteristic for that system. These patterns can then be imposed on the model for the target reservoir using a growth-based stochastic simulation technique proposed in this paper. These stochastic models can be constrained to all available information in the form of conditioning well data, seismic maps, rock mechanical strength data etc.

Although the general framework for fracture classification and simulation has been presented, many specific issues pertaining to fracture characterization remain unresolved. Variations in connectivity measures corresponding to subtle variations in lithology have to be further studied. The issue of 3-D analog model construction from multiple 2-D outcrop exposures is a

challenging one and requires considerable effort as evidenced in another paper²⁶ in this proceeding. Finally, physical parameters that control fracture propagation such as variations in rock strength, proximity to a fault have to be quantified in terms of their impact on the conditional probability distribution controlling fracture growth. Further research on integration of such information is needed.

Acknowledgement

Financial support received from US Oilfield Corporation is gratefully acknowledged.

References

1. Nelson, Ronald A., *Geologic Analysis of Naturally Fractured Reservoirs*, Gulf Publishing Company, Houston, Texas, 1985.
2. Handin, J. and Hager, R.V., "Experimental determination of sedimentary rocks under confining pressure : Tests at room temperature in dry samples", *AAPG Bulletin*, Vol. 41, pp 1-50, 1957.
3. Stearns, D.W. and Friedman, M., *Reservoirs in Fractured Rock*, AAPG Memoir 16, pp 82-100, 1972.
4. Stearns, D.W., "Macrofracture patterns on Teton anticline, Northwest Montana", *American Geophysical Union Transactions*, Vol. 45, pp 107-108, 1964.
5. Yamaguchi, T., "Tectonic study of Rock Fractures", *Journal of Geological Society of Japan*, Vol. 71, No. 837, pp. 257-275, 1965.
6. Charlesworth, H.A.K., "Some observations on the age of jointing in macroscopically folded rocks", in *Kink Bands and Brittle Deformation*, A.J. Baer and D.K. Norris editors, Geological Survey of Canada, Paper 68-52, pp. 125-135, 1968.
7. Stearns, D.W., "Mechanisms of Drape Folding in the Wyoming Province", *Guidebook 23rd Annual Field Conference*, Wyoming Geological Association, pp. 125-143, 1971.
8. Nelson, R.A. and Stearns, D.W., "Interformational Control of Regional Fracture Orientations", in *Rocky Mountain Association, Field Trip Guidebook, Exploration Frontiers*, pp. 95-101, 1977.
9. Price, N.J., "The Development of Stress Systems and Fracture Patterns in Undeformed Sediments", *Proceedings of the 3rd International Congress on Rock Mechanics*, pp. 487-496, 1974.
10. Netoff, D.I., "Polygonal Jointing in Sandstone near Boulder, Colorado", *Mountain Geologist*, Vol. 8, No.1, pp. 17-24, 1971.
11. Picard, M.D., "Oriented Linear-Shrinkage Cracks in Green River Formation (Eocene), Raven Ridge Area, Uinta Basin, Utah", *Journal of Sedimentary Petrology*, Vol. 36, No. 4, pp. 1050-1057.
12. Peck, D.L. and Minakami, T., "The Formation of Columnar Joints in the Upper part of Kilauean Lava Lakes, Hawaii", *Geological Society of America Bulletin*, Vol. 79, No. 9, pp. 1151-1166, 1968.
13. Nelson, R.A., "An Experimental Study of Fracture Permeability in Porous Rocks", in *Proc. of the 17th*

Symposium on Rock Mechanics, Snowbird, Utah, pp. 8, 1976.

14. Nelson, R.A., "Natural Fracture Systems, Description and Classification", *AAPG Bulletin*, Vol. 63, No. 12, pp. 2214-2221, 1979.
15. Deutsch, C.V. and Journel, A.G., *GSLIB: Geostatistical Software Library and User's Guide*, Oxford University Press, New York, N.Y., 1992.
16. Alabert, F. and Journel, A.G., "New Method for Reservoir Mapping", *Journal of Petroleum Technology*, pp. 212-218, 1990.
17. Deutsch, C.V., *Annealing Techniques Applied to Reservoir Modeling and the Integration of Geological and Engineering (Well Test) Data*, Ph.D. Thesis, Stanford University, Stanford, CA, 1992.
18. Baecher, G.B., Einstein, H.H. and Lanney, N.A., "Statistical Descriptions of Rock Properties and Sampling", *Proc. Of the 18th U.S. Symposium on Rock Mechanics*, pp. 5C1.1-5C1.8, 1977.
19. Billaux, D., Chiles, J.P., Hestir, K. and Long, J., "Three Dimensional Statistical Modeling of a Fractured Rock Mass: an Example from the Anay-Agueres Mine", *International Workshop on Forced Fluid Flow through Fractured Rock Masses*, Vol. 26, No. 3-4, pp. 281-299, 1989.
20. Guardiano, F. and Srivastava, R.M. "Multivariate Geostatistics: Beyond Bivariate Moments", in *Geostatistics Troia '92*, A. Soares editor, Kluwer Academic Publisher, Vol. 1, pp. 133-144, 1992.
21. Journel, A.G., "Geostatistics: Roadblocks and Challenges", in *Geostatistics Troia '92*, A. Soares editor, Kluwer Academic Publisher, Vol. 1, pp. 213-224, 1992.
22. Caers, J., "Stochastic Reservoir Characterization using Multiple-point Statistics", in *Proc. of the IAMG 99, Fifth Annual Conference of the International Association for Mathematical Geology*, Lippars, S.G. et al editors. Vol. 2, pp. 467-472.
23. Strebelle, S., "Conditional Simulation of Complex Geological Structures using Multiple-point Statistics". *Mathematical Geology*, v. 34, p. 1-22, 2002.
24. Gringarten, E., *Geometric Modeling of Fracture Networks*, Ph. D. Thesis, Stanford University, Stanford, CA, 1997.
25. Wang, L., "Modeling Complex Reservoir Geometries with Multiple-point Statistics", *Mathematical Geology*, Vol. 28, No. 7, 1996.
26. Merchan, S., Srinivasan, S. and Meyer, R., "Characterization of estuarine-shore type reservoirs using outcrop analogs and modeling of flow using a non-uniformed coarsened grid", in this proceeding.

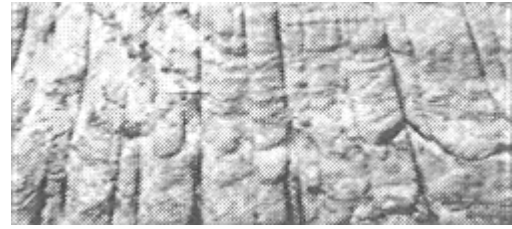


Figure 1: Regional fracture patterns found in Jurassic Navajo sandstone, Lake Powell, southeastern Utah¹³

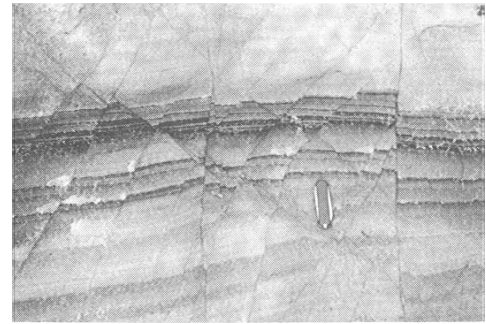


Figure 2: Conjugate shear fractures corresponding to a tectonic fracture system found in an outcrop from Wyoming.



Figure 3: Example of desiccation cracks observed in mud.

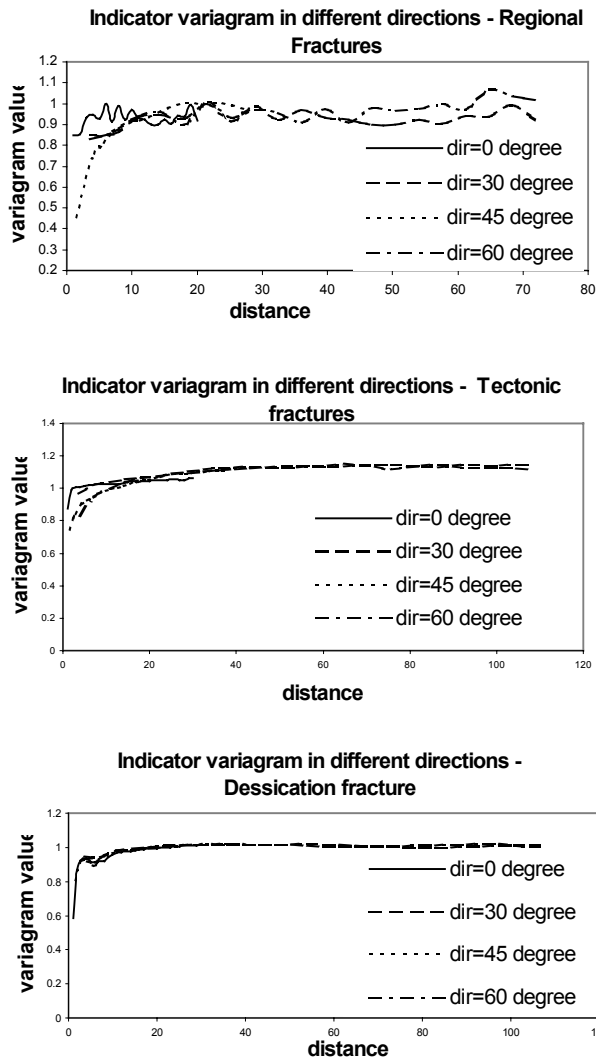


Figure 4: Indicator variograms in different directions computed on the three types of fracture models shown in Figures 1-3.

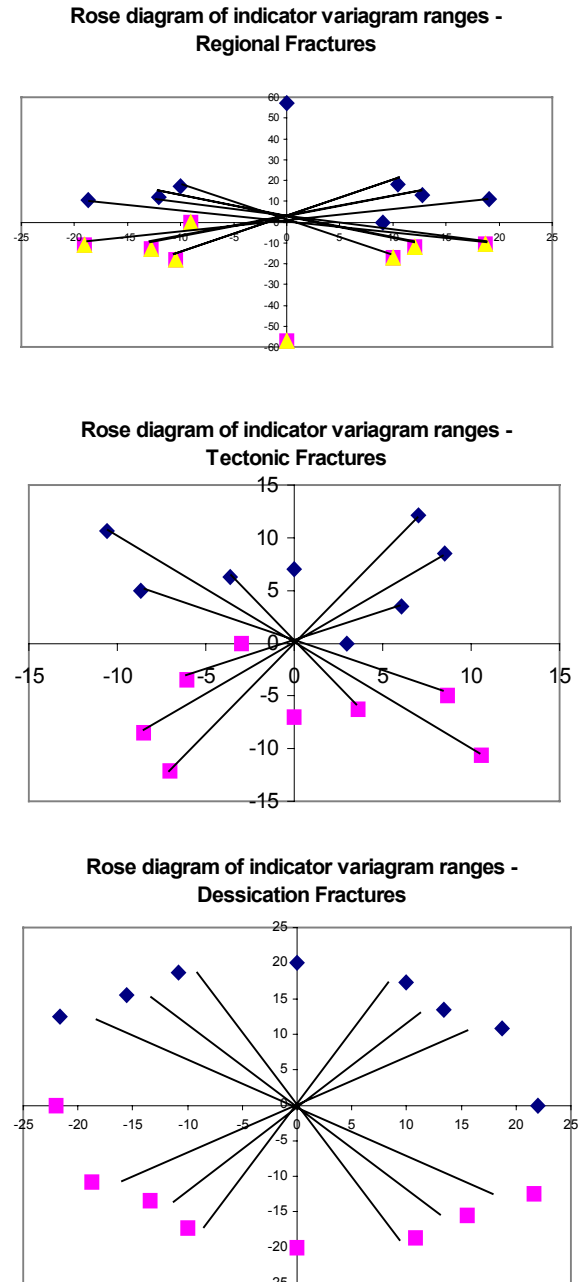


Figure 5: Rose diagram summarizing the indicator variogram ranges in different directions.

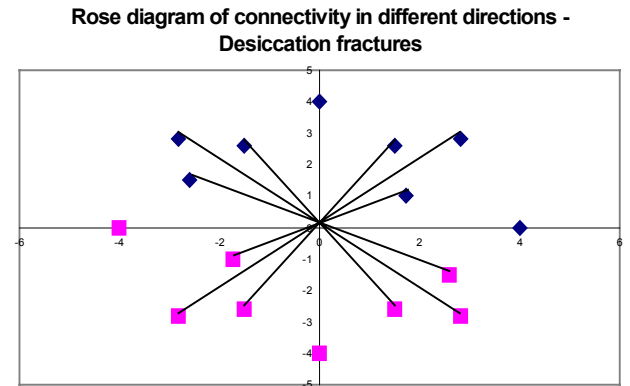
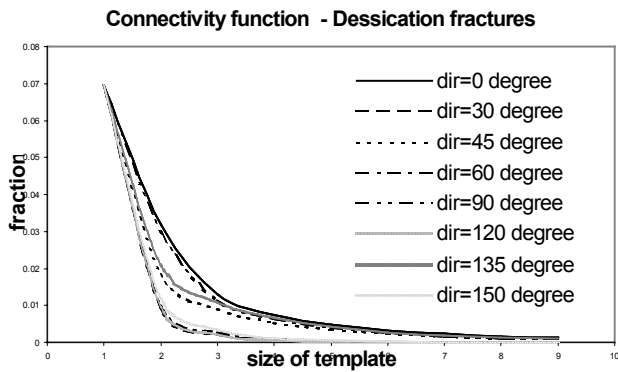
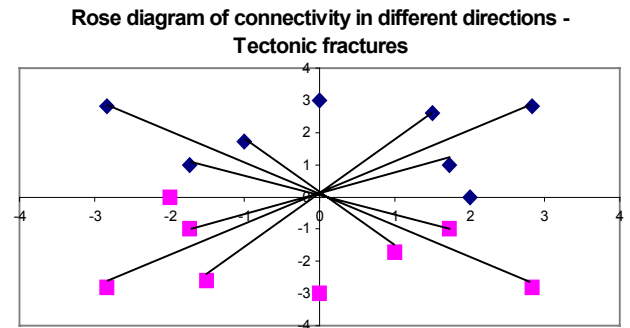
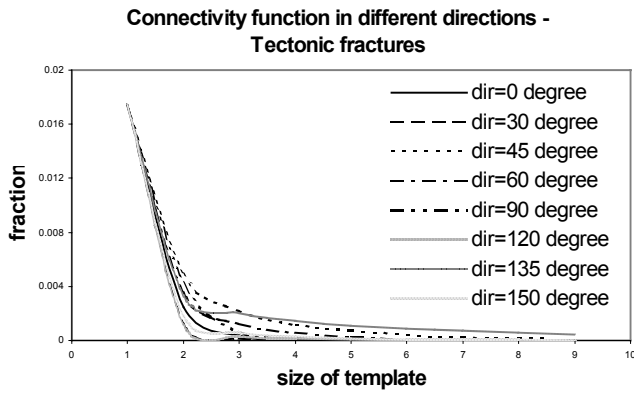
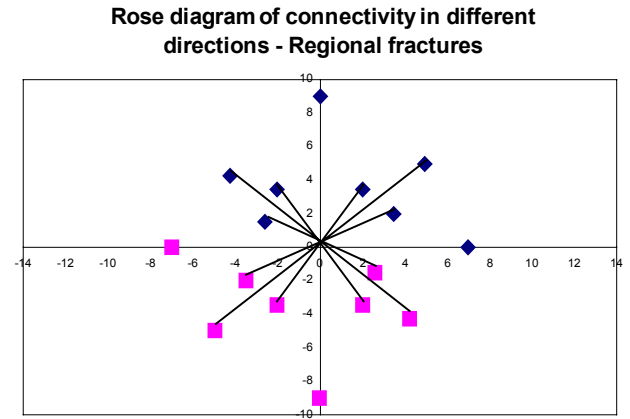
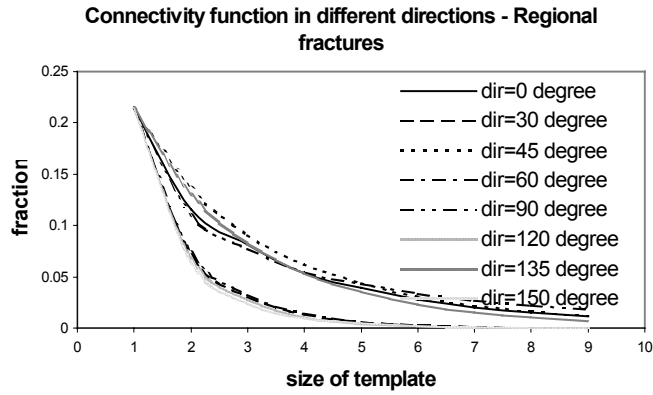


Figure 6: Connectivity function calculated on the three types of fracture models in different directions.

Figure 7: Rose diagram of range of connectivity function in different directions computed for the three types of fractures. The range is defined as the size of the lag template over which the connectivity value drops to 10% of the initial connectivity value.

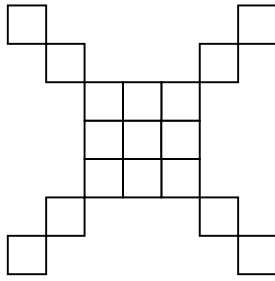


Figure 8: Spatial 2-D template used for computing multiple point histograms.

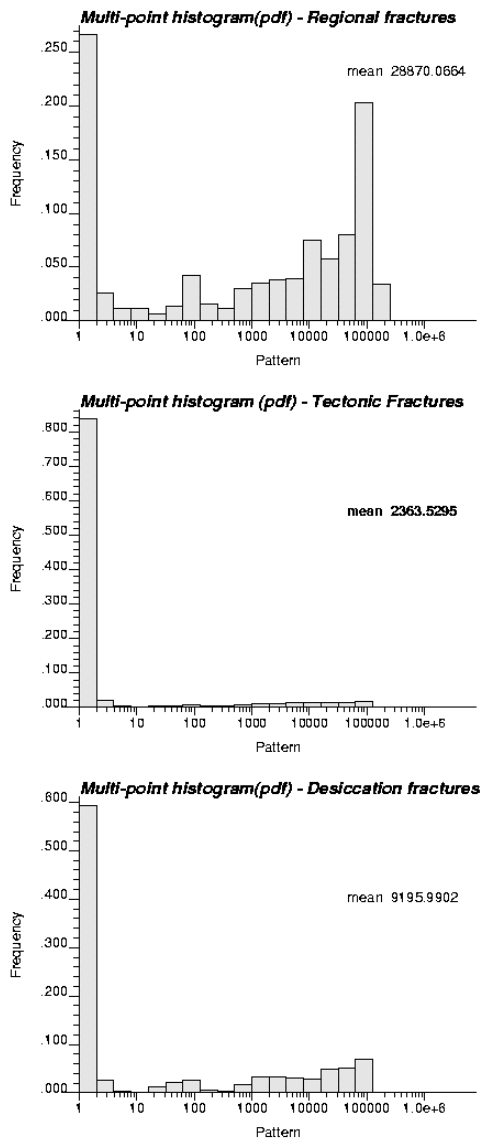


Figure 9: Multi-point histogram corresponding to the three different fracture systems.

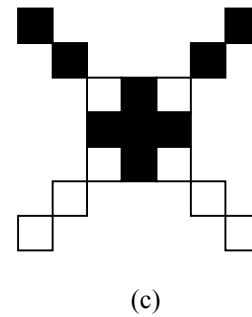
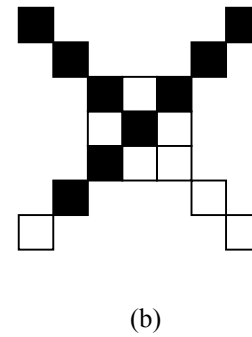
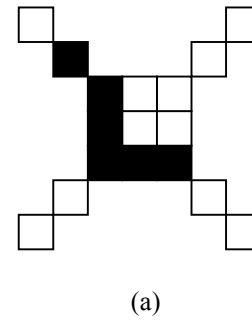


Figure 10: Pattern corresponding to the mean of the multiple point histogram for each fracture system. (a) Pattern detected for regional fracture system consistent with the predominantly N-S and E-W orientation of fracture (b) Pattern detected for shear fracture system consistent with pattern expected for fractures associated with normal faults (c) Pattern corresponding to desiccation cracks, fracture exhibit no predominant orientation.

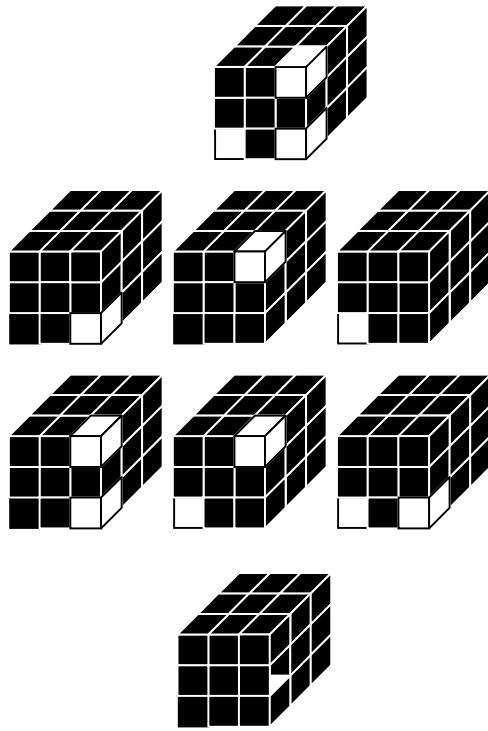


Figure 11: A 27-point 3-D spatial template with 24 nodes identified as fractures. The various possible combinations of events that are possible at the remaining 3 nodes are portrayed.

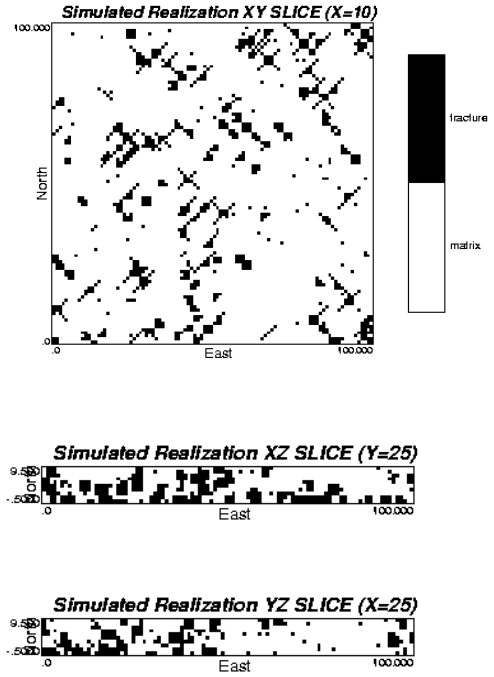


Figure 13: Slices through one simulated realization. The simulated model is constrained to well data and global proportion of fractures equal to 20%.

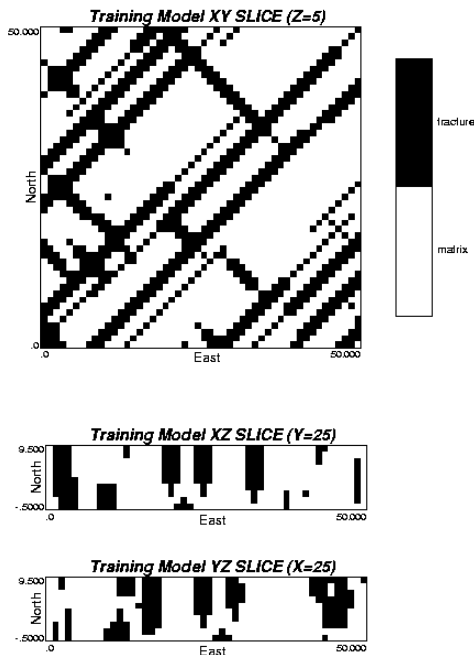


Figure 12: Slices through the training fracture model used to retrieve multiple-point conditional probabilities. Proportion of fractures in the training model is 50%.

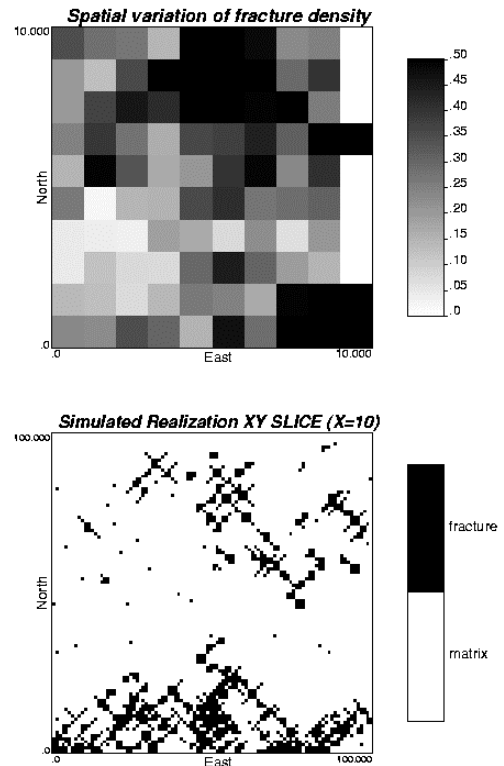


Figure 14: Spatial variation of fracture density and a horizontal slice through simulation constrained to the areal proportion.